JOURNAL OF AGRICULTURAL AND FOOD CHEMISTRY
ARTICLE

J. Agric. Food Chem. 2009, 57, 10399–10407 10399
DOI:10.1021/jf9016948

Structure and Chemical Composition of Layers Adsorbed at Interfaces with Champagne

V. Aguié-Béghin,*,† Y. Adriaensen,‡ N. Péron,§ M. Valade,∥ P. Rouxhet,‡ and R. Douillard†

†INRA-UMR 614 Fractionnement des Agro-Ressources et Environnement (FARE) INRA/Université de Reims Champagne Ardennes, Centre de Recherche en Environnement et Agronomie, 2 Esplanade R. Garros, BP 224, F-51686 Reims, France, ‡Unité de Chimie des Interfaces, Université Catholique de Louvain, Louvain-la-Neuve, Belgium, §Departement of Chemistry, University of Durham, United Kingdom, and ∥Comité Interprofessionnel du Vin de Champagne, 5 rue Henri-Martin, BP 135, 51204 Epernay Cedex, France

The structure and the chemical composition of the layer adsorbed at interfaces involving champagne have been investigated using native champagne, as well as ultrafiltrate (UFch) and ultraconcentrate (UCch) obtained by ultrafiltration with a 10^4 nominal molar mass cutoff. The layer adsorbed at the air/liquid interface was examined by surface tension and ellipsometry kinetic measurements. Brewster angle microscopy demonstrated that the layer formed on polystyrene by adsorption or drop evaporation was heterogeneous, with a domain structure presenting similarities with the layer adsorbed at the air/liquid interface. The surface chemical composition of polystyrene with the adlayer was determined by X-ray photoelectron spectroscopy (XPS). The contribution of champagne constituents varied according to the liquid (native, UFch, and UCch) and to the procedure of adlayer formation (evaporation, adsorption, and adsorption + rinsing). However, their chemical composition was not significantly influenced either by ultrafiltration or by the procedure of deposition on polystyrene. Modeling this composition in terms of classes of model compounds gave approximately 35% (w/w) of proteins and 65% (w/w) of polysaccharides. In the adlayer, the carboxyl groups or esters represent about 18% of carbon due to nonpolypeptidic compounds, indicating the presence of either uronic acids in the complex structure of pectic polysaccharides or of polyphenolic esters. This structural and chemical information and its relationship with the experimental procedures indicate that proteins alone cannot be used as a realistic model for the macromolecules forming the adsorption layer of champagne. Polysaccharides, the other major macromolecular components of champagne wine, are assembled with proteins at the interfaces, in agreement with the heterogeneous character of the adsorbed layer at interfaces.

KEYWORDS: Adsorption; champagne; proteins; polysaccharides; X-ray photoelectron spectroscopy; ellipsometry; ultrafiltration; surface tension; interface

INTRODUCTION

A collar of fine bubbles at the surface of a sparkling wine is an organoleptic property of utmost importance for champagne. It is the first perception of the wine taster. The ring of bubbles is the result of the effervescence originating from the nucleation sites which may be imperfections of the glass surface or preexisting gas cavities trapped at the surface (*1*). The nucleation is followed by the growth and rise of bubbles, followed by their migration to the glass periphery, on the one hand, and their disappearance by resorption, bursting and coalescence on the other hand (*2*, *3*). The state of the resulting ring is linked with the rate of formation and of disappearance of bubbles. The rate of the growth of bubbles (*4*) and the stability of bubbles in the collar (*5*) are usually related to the occurrence and to the properties of an adsorption layer formed at the gas/wine interface (*6*).

The adsorption layers were shown to be mostly composed of macromolecules with a molar mass in the range 10^4 to 10^5 g/mol (*5*). The macromolecules originate from grape and yeast and may be proteins (5−10 mg/L in wine) and polysaccharides (200−500 mg/L in wine) (*7*, *8*). They are soluble in the hydro-alcoholic solution and cause together with ethanol (close to 12,5% (v/v)) a decrease of the surface tension down to about 47 mN/m. It was shown by Brewster angle microscopy that this interface has a domain structure (*9*). Nevertheless, the chemical nature and the respective role of these compounds are not known. Preliminary observations are in favor of the occurrence of proteins in the layer (*8*, *10*). To test this hypothesis, a grape invertase of 62 000−64 000 molar mass has been purified (*11*) and characterized by the surface properties conferred to model hydro-alcoholic systems (*12*). The thermodynamic property analysis of the layer has shown that invertase alone

*Corresponding author. Tel: 33 3 26 77 35 95. Fax: 33 3 26 77 35 92. E-mail: Veronique.Aguie@reims.inra.fr.

Published on Web 10/08/2009

cannot be the major component of the adsorption layer formed at the gas/champagne wine interface (*5*, *12*).

In the present study, the chemical composition of the surface active molecules present in champagne has been investigated. Therefore, the examination of the gas/champagne interface by surface tension measurement and ellipsometry was combined with the X-ray photoelectron spectroscopy (XPS) analysis of a polystyrene surface conditioned with the champagne and dried. The analysis of solid surfaces by XPS is based on irradiation with an X-ray beam under high vacuum and emission of electrons, the kinetic energy of which is analyzed (*13*). This provides, after adequate calibration, a spectrum plotted as a function of the binding energy (in eV) of the emitted photoelectrons. Each peak is characteristic of a given energy level (1s, 2s, 2p ...) of a given element. The binding energy is influenced by the chemical environment of the element and thus provides information on the chemical functions in which it is incorporated. Owing to inelastic scattering of electrons in a solid, the information collected concerns the outermost molecular layers (thickness of the order of 5 nm) at the surface. Application of the method to food cakes has revealed that surface accumulation increases in the order proteins < triglycerides < phospholipids (*14*). Its application to spray-dried powders revealed a surface enrichment in phospholipid relative to albumine and its dependence on spray drying conditions (*15*). The analysis of spray-dried dairy powders (*16*) revealed a surface enrichment in lipids with respect to lactose and its influence on powder wetting time. Surface enrichment in lipids during storage of spray-dried phosphocaseinate was also observed by XPS and found to increase the wetting time (*17*).

As the polystyrene surface is not polar, it is expected that the air/liquid and polystyrene/liquid interfaces present similarities regarding the driving forces ruling the adsorption of nonvolatile organic compounds. In contrast with high energy polar substrates, the polystyrene surface is not appreciably contaminated by organic compounds which complicate the interpretation of the C_{1s} peak shape (*18*). As compared with saturated polyolefins, it has the advantage that the C_{1s} shake up is a marker for the contribution of the substrate to the recorded spectrum.

The three techniques used here are complementary for the investigation of this system. Tensiometry provides a physicochemical characterization of the air/liquid interface. Ellipsometry and Brewster angle microscopy (BAM) give information on the optical properties of interfacial thin layers (*19*−*21*) with the advantage that they may be used for both the air/liquid and the air/solid interfaces, and provide information on the adlayers in terms of evolution with time and domain organization. XPS provides information in terms of chemical composition but can only be applied to an air/solid interface.

MATERIALS AND METHODS

Samples. The champagne wine was produced from a Chardonnay vine variety grown by CIVC (Comité Interprofessionnel du Vin de Champagne, Epernay, France). Ultrafiltration (ultraconcentration) of the base wine was performed by tangential ultrafiltration on a 1.8 m^2 hollow fiber device (Inceltech, Toulouse, France) with a cutoff nominal molar mass of 10^4 g/mol as described previously (*5*). During the ultrafiltration, the speed of the peristaltic pump was adjusted to achieve a 3-fold ultraconcentration of the wine, and the transmembrane pressure was maintained at 0.7 atm. All of the samples were stored in 0.75 L bottles. The second fermentation was achieved by adding yeast and 18 g of sugar to each bottle, which was finally closed by a gastight plug. The concentrations of ethanol and carbon dioxide increased during that fermentation, yielding sparkling wine. After the expulsion of lees, the bottles were sealed with capsules and stored at 4 °C. The concentration of compounds with a molar mass above 10^4 g/mol is about 151 mg/L for the sample originating from the native base wine (native) (*22*), about three times higher for the one obtained from ultraconcentrate base wine (UCch) and nearly zero for the one issued from ultrafiltrate base wine (UFch). Three samples (corresponding to three bottles) of each champagne were prepared for XPS analysis and surface property measurements. All experiments were made with partially degassed champagne by opening the bottle 3 days before XPS analysis or under nitrogen flux before optical and tensiometric measurements. Thus, the structural and chemical composition of adsorbed layers were obtained without fluid motion due to the rising gas columns in contrast with that in ref *23*.

Adsorbed Layer at the Air/Champagne Interface. Surface tension and ellipsometry measurements were performed as described previously (*5*). The sample was poured into the vessel (a glass petri dish 60 mm in diameter) just before data acquisition.

Tensiometry. Surface tension was measured using a tensiometer from IT Concept (Longessaigne, France) (*24*, *25*). Only the drop method was used in this work, similar to the one previously described (*26*) . For its operation, an axisymmetric drop was formed at the tip of a Teflon-coated needle of a syringe, the plunger of which was driven by an electric motor. This experiment was performed in a confining cell (~250 mL) with two parallel windows for optical measurements, thermostated at 20.0 ± 0.1 °C. Its bottom was coated with a few milliliters of wine to allow equilibration with saturating vapors and to avoid evaporation from the drop. The plunger of the syringe was allowed to enter through a toric seal, ensuring gas tightness of the cell. The image of the drop was taken with a CCD camera and digitized. The surface tension, γ, was determined by analyzing the profile of the drop according to the Laplace equation (*24*). To begin the measurements, three drops were quickly expelled before forming the measuring drop. The latter was then formed within 1 s, and the surface tension was monitored as a function of time. This procedure allowed a good reproducibility, with a standard deviation of the measured surface tension less than 0.1 mN/m (*26*). Since ethanol (~10.8% v/v) adsorbs quickly and lowers the surface tension down to 46.9 mN/m, samples used for tensiometry were diluted four times with water in order to reveal more clearly the surface active properties of other wine compounds as detailed in ref *26*.

Ellipsometry. The evolution of the Brewster ellipticity was monitored as a function of time after the formation of the liquid−gas interface. The two ellipsometric angles Ψ and Δ are linked to the two reflectivity coefficients r_p and r_s, in the direction parallel and perpendicular to the incidence plane, respectively, by (*21*):

$$\frac{r_p}{r_s} = \tan \Psi \exp(i\Delta) \quad (1)$$

The reflectivity coefficients were measured at a fixed wavelength which corresponds to the Brewster conditions for the substrate liquid defined by $\Delta = \pm \pi/2$. The ellipticity coefficient, $\bar{\rho}_B$, is then defined by

$$\bar{\rho}_B = \tan \Psi \sin \Delta \quad (2)$$

In the case of the Fresnel interface (ideal case of an interface between two transparent media without roughness), the ellipticity is $\bar{\rho}_B = 0$. Experimentally, the coefficient r_p is not zero and the ellipticity passes through a positive minimum value, which is due to the roughness of the interface (thermally induced capillary waves at the liquid surface). In the case where an adsorption layer occurs with a thickness d, much lower than the wavelength λ, and where the optical anisotropy of the interface can be neglected, $\bar{\rho}_B$ is the sum of two contributions, the roughness positive term $\bar{\rho}_r$ and the adsorption layer negative term $\bar{\rho}_d$ for a layer with a refractive index larger than that of the liquid (*20*). From the Drude equation and assuming that the refractive index of the layer is constant and that the refractive index of air is unity, the Brewster angle ellipticity is proportional to the surface concentration when an adsorption layer forms at the air/liquid interface (*27*).

The measurements were performed using a spectroscopic phase modulated ellipsometer (UVISEL, Jobin Yvon, Longjumeau, France) equipped with a xenon arc source, as described previously (*27*, *28*). Both the polarizer and the analyzer were set to the 45° configuration angle. The photoelastic modulator activated at a frequency of 50 kHz was set to 0°. The diameter of the light beam was set to 1 mm. The incidence angle was set to 53.6°. All measurements were done in an air-conditioned room at 20 ± 1 °C.

Polystyrene with an Adsorbed or Deposited Layer. Opened bottles were stored at 4 °C during 72 h before XPS analysis. Three different procedures of conditioning polystyrene plates (0.5 cm × 0.5 cm, cleaned by sonication in isopropanol) were used. The first one (ads) was an immersion during 2 h of the polystyrene plate in 10 mL of champagne previously degassed for 15 min by nitrogen bubbling. The second procedure (rins) started as the first one, but after immersion, the polystyrene plate was rinsed consecutively 5 times by using the following protocol which led to a dilution by a factor 10^5: removal of 9 mL of liquid, addition of 9 mL of ultrapure water, rest for 15 min. In the third procedure (evap), 30 μL of champagne was spread on the polystyrene plate and dried during 12 h in ambient conditions. Samples of types ads and rins were dried in nitrogen flow and stored for 6 h in a desiccator at room temperature before analysis.

Brewster Angle Microscopy (BAM). The technique of Brewster angle microscopy (BAM) uses the properties of the Brewster reflection and of the ellipticity coefficient $\overline{\rho}_B$ to observe micrometer scale inhomogeneities due to variations in the thickness and in the refractive index of the adsorbed layer. The linear p-polarized light incident at the Brewster angle of the substrate is set at 0°, and the relation between the two reflectivity coefficients is

$$r_p = ir_s\overline{\rho_B} \quad (3)$$

On the pure substrate, the incident light beam is not reflected ($r_p = 0$). The presence of the monolayer modifies the optical properties ($r_p \neq 0$). The reflectance R ($= I_r/I_0$) of thin films is proportional to $\overline{\rho}_B{}^2$ and then to the square of the adsorbed layer thickness (d^2). As a consequence, the uncovered substrate appears dark in the BAM images, whereas all parts covered by thin layers appear bright. A decisive advantage of this method is that fluorescent labeling is not required, as is the case in fluorescent microscopy, and that internal structures of domains can also be assessed.

BAM measurements were performed on samples prepared according to procedures ads and evap using an Optrel Multiskop ellipsometer (*29*, *30*) (Optrel, Berlin, Germany, www.optrel.de). The laser arm and the CCD camera arm were mounted on a goniometer. The laser arm contains a 50 mW Nd:YAG laser with a wavelength of 5320 Å and a polarizer, while the CCD camera arm contains an analyzer, a projective lens, and an objective (10×, Numerical Aperture 0.28). Images were taken with a resolution of 1.2 μm.

XPS Analysis. The XPS analysis was performed with a Kratos Axis Ultra (Kratos Analytical, UK) as described before (*14*): pass energy of 160 and 40 eV for the survey spectrum and individual spectra, respectively; analysis area 700 μm × 300 μm; collection angle between the normal to the sample surface and the direction of the photoelectron collection 0°; data treatment with Casa XPS (Casa Software Ltd.); and molar concentration ratios calculated using sensitivity factors and transmission function proposed by the manufacturer. The peaks were recorded in the following sequence: survey spectrum, C_{1s}, O_{1s}, N_{1s}, Si_{2p}, and C_{1s}, again to check for the absence of sample degradation and for charging stability during analysis. The binding energy scale (eV) was set by fixing to the C1s component attributed to carbon only bound to carbon and hydrogen [C-(C,H)] at 284.8 eV. The C_{1s} and N_{1s} peaks were decomposed using a linear baseline and a component shape given by a Gauss−Lorentz product function 70:30. Further details will be given with the results.

RESULTS

Adsorbed Layer at the Air/Champagne Interface. Ellipsometric measurements were performed with samples directly representative of the wine. The evolution of Brewster ellipticity as a function of time, subsequent to pouring the samples into the petri dish, is presented in **Figure 1**. The native sample exhibits a fluctuating signal between a positive $+2 \times 10^{-3}$ and a negative value -6×10^{-3} during 750 s, followed by a stable value near -8×10^{-3}. Positive values revealing surface roughness without adsorption layer are also observed for the UFch at short times. These signal evolutions indicate that the macromolecules progressively form an adsorbed layer which, at first, is not homogeneous at the scale of the light beam (*5*). In the case of UCch, a different pattern was observed. In a few seconds, the Brewster ellipticity reached a stable value at -9×10^{-3}, which was close to the equilibrium value obtained with another experimental champagne of the 2004 vintage (*31*), indicating the fast formation of an adsorbed layer. The signal of numerous sample batches often exhibits large fluctuations which correspond to heterogeneities of the mobile adsorption layer (the layer may move quite freely at the interface) (*31*). The mean value of the signal $\langle|\overline{\rho}_B|\rangle$ during the 30 min kinetics was determined from the data in **Figure 1**, according to ref *31* and found to be $3 \times 10^{-3} \pm 2 \times 10^{-3}$ for UFch, $6.4 \times 10^{-3} \pm 2 \times 10^{-3}$ for native, and $8.5 \times 10^{-3} \pm 0.9 \times 10^{-3}$ for UCch. Despite the variations, it is clear that the value was more negative as the concentration of macromolecules in champagne increased.

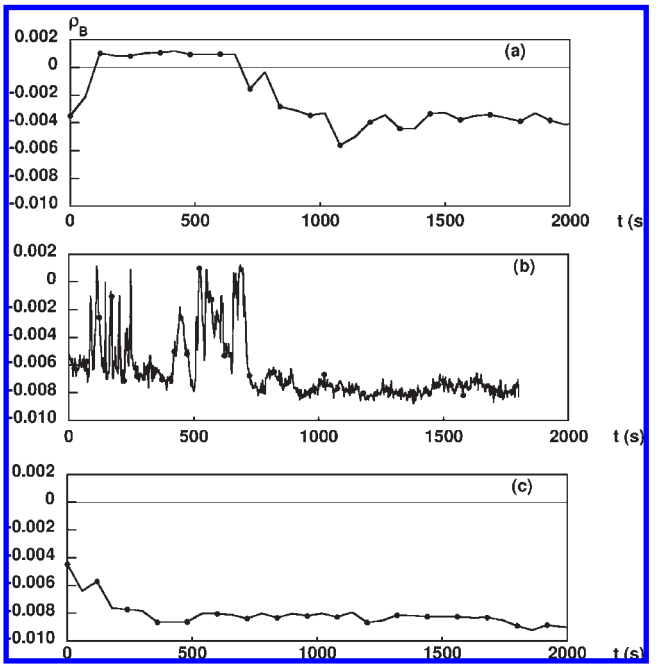

Figure 1. Evolution of the Brewster ellipticity, $\overline{\rho}_B$, at the interface between air and (**a**) UF champagne, (**b**) native champagne, and (**c**) UC champagne.

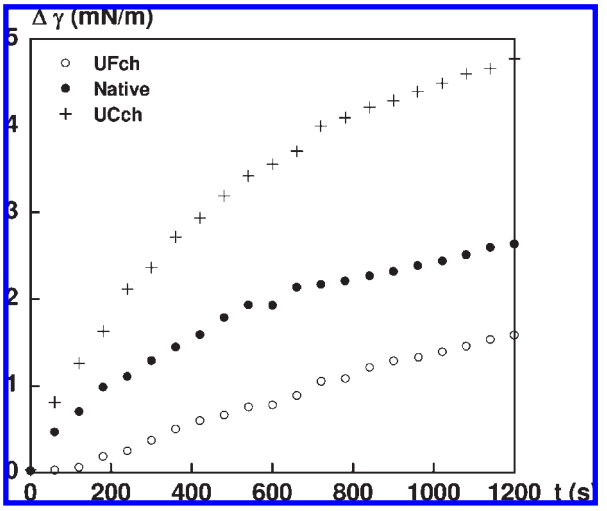

Figure 2. Evolution of the surface tension at the interface between air and champagne diluted four times with water. Results are shown as $\Delta\gamma$, the difference between surface tension just after drop formation and surface tension at time t (s.d. 0.1 mN/m).

The surface tension of diluted UFch, native, and UCch champagnes was lowered from 1 to 5 mN/m in a few minutes, the rate of variation increasing according to the order UFch < native < UCch (**Figure 2**), which demonstrates that surface active compounds adsorb at the air/liquid interface.

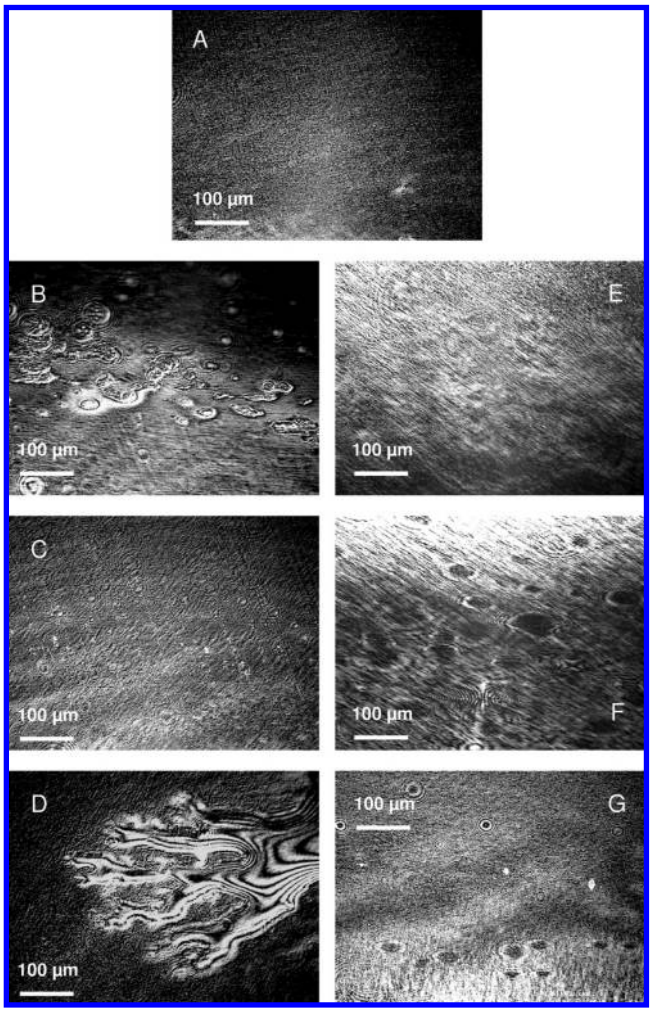

Figure 3. Brewster angle microscopy images of polystyrene as such (**A**), conditioned according to ads(**B**−**D**), and conditioned according to evap-(**E**−**G**).

These measurements show that all samples contain surface active macromolecules. They are clearly correlated with the concentration of macromolecules of the wine samples: the rate of formation of the adsorbed layer at the air/liquid interface and the adsorbed amount increase with the concentration of macromolecules.

Layers Adsorbed or Deposited on Polystyrene. The bare polystyrene plates examined by Brewster angle microscopy show a homogeneous and smooth surface. After being submitted to adsorption in contact with native champagne (procedure ads) or to spreading and evaporation of a drop (procedure evap), the plates exhibit a domain structure of the adsorbed layer (**Figure 3B**−**D**) or the evaporation residue of nonvolatile components (**Figure 3E**−**G**). Owing to the heterogeneity of the adlayer, it was not possible to go further in determining the thickness and refractive index of the layers by ellipsometry. It may be noted that the layer adsorbed on polystyrene (ads) has a domain structure which presents some similarity with the domain structure observed previously at the air/champagne interface (*9*). This supports the idea that the layer formed on polystyrene ressembles that formed at the air interface.

Two independent sets of XPS analyses were performed on plain polystyrene and on polystyrene conditioned with the 3 samples of champagne using the 3 different procedures. The molar concentration ratios of all detected elements, expressed with respect to carbon, are given in **Table 1**, and representative spectra are shown in **Figure 4**. Note that hydrogen is not detected by XPS; the other elements typical of biological materials (P, Na, and S), which were not detected, were below the detection limit of about 0.001 times the carbon concentration (*13*). Besides carbon, nitrogen, and oxygen, potassium was detected for some samples. Silicon was detected at a low concentration for all samples (Si/C in the range of 0.001 to 0.009) and may be attributed to silane or silica because of ambient contamination or to silicate originating from glass vessels. Its concentration is too low to interfere with the data exploitation developed below.

When the molar concentration ratios with respect to carbon are considered, it must be kept in mind that the carbon peak may

Table 1. Surface Composition of Polystyrene Washed with Isopropanol and Conditioned with Different Champagne Samples (UFch, Native, and UCch) Using Different Procedures (evap, ads, and rins): Molar Concentration Ratio, with Respect to Total Carbon, of Elements and of Carbon and Nitrogen Species Characterized by the Indicated Binding Energy (eV) of the XPS Peak

		elements			chemical species					
sample		O	N	K	C-(C,H)	C-(O,N)	C=O	COO	N_{am}	N_{pos}
					284.8	286.2	287.9	289	400	401.8
UFch	evap	0.082	0.013	bdl	0.830	0.107	0.016	0.011	0.010	0.003
	evap	0.646	0.117	0.008	0.226	0.493	0.139	0.134	0.095	0.022
	ads	0.086	0.018	bdl	0.833	0.098	0.016	0.013	0.015	0.003
	ads	0.406	0.061	0.007	0.551	0.228	0.102	0.083	0.048	0.013
	rins	0.082	0.019	bdl	0.838	0.105	0.017	0.01	0.019	bdl
	rins	0.135	0.038	bdl	0.752	0.133	0.044	0.035	0.035	0.003
native	evap	0.549	0.093	0.003	0.310	0.458	0.123	0.106	0.074	0.019
	evap	0.542	0.098	0.007	0.226	0.517	0.142	0.107	0.082	0.016
	ads	0.121	0.023	0.003	0.791	0.127	0.029	0.021	0.020	0.003
	ads	0.109	0.022	bdl	0.779	0.126	0.035	0.024	0.019	0.003
	rins	0.171	0.025	bdl	0.744	0.187	0.034	0.025	0.023	0.002
	rins	0.226	0.042	bdl	0.707	0.145	0.073	0.047	0.039	0.003
UCch	evap	0.516	0.104	bdl	0.305	0.448	0.140	0.103	0.088	0.016
	evap	0.621	0.110	0.003	0.262	0.496	0.137	0.102	0.092	0.018
	ads	0.156	0.030	0.002	0.774	0.148	0.037	0.023	0.026	0.004
	ads	0.582	0.083	0.008	0.362	0.416	0.109	0.104	0.060	0.023
	rins	0.152	0.033	bdl	0.743	0.164	0.043	0.029	0.031	0.002
	rins	0.209	0.036	0.004	0.693	0.179	0.058	0.050	0.033	0.003
polystyrene		0.013	bdl	bdl						

contain a contribution not only of the champagne constituents but also of the polystyrene substrate. As a matter of fact, the high

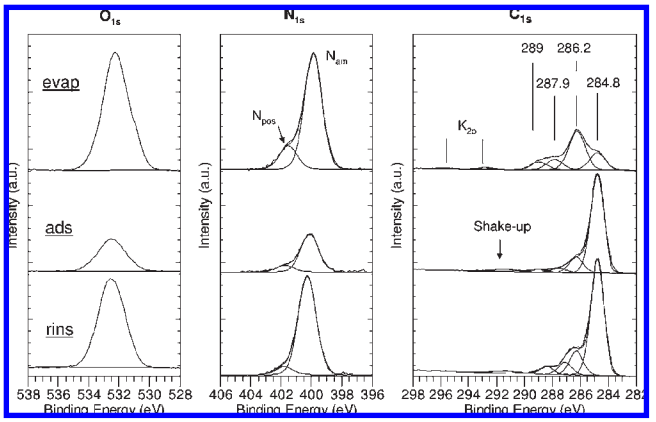

Figure 4. Representative O_{1s}, N_{1s}, and C_{1s} peaks of polystyrene conditioned with native champagne according to the indicated procedure.

Table 2. Binding Energy and Assignment of XPS Peaks and Peak Components (*18*)

binding energy (eV)	assignment	
284.8	**C**-(C,H)	hydrocarbon
286.2	**C**-(O,N)	alcohol, ether, amide, amine
287.9	**C**=O; O-**C**-O	amide, acetal, hemiacetal, carboxylate
289.0	O-**C**=O	ester, carboxyl
291.5		shake up peak of polystyrene
400.0	N_{am}	amide, amine
401.8	N_{pos}	ammonium, protonated amine
531.2[a]	**O**=C	carboxylate, ester, carbonyl, amide
531.8[a]	O=C-**O**-(C,H)	ester, carboxyl
532.6[a]	C-**O**-C; C-**O**H	alcohol, ether
533.4[a]	O=C-**O**-(C,H)	ester, carboxyl

[a] Expected; peak not decomposed.

variability observed between the two sets of results in three cases (UFch-evap, UFch-ads, and UCch-ads) is attributed to a variation of the adlayer (adsorbed or deposited layer) thickness or to an overlap of the analyzed zone on the noncoated polystyrene. This is supported by the fact that a low O and N concentration is accompanied by a high proportion of the C-(C,H) component in the C_{1s} peak (**Table 2**) and with the observation of the shake up, as illustrated by sample ads in **Figure 4**. A variation of the adlayer thickness is in agreement with the domain structure observed by BAM (**Figure 3**). The variability may also be due to experimental factors: error in selecting the analyzed zone, targeted as the trace of the drop submitted to evaporation (UFch-evap), and heterogeneity created by the nitrogen flow used for quick drying (UFch-ads, UCch-ads). Such variability does not impair the conclusions of the present work. However, it points to the need to better control the influence of drying in a broader use of the method.

Correlations between molar concentration ratios provide valuable information which is not affected by the amount of champagne compounds present in the zone probed by XPS. The plot of molar ratios N/C versus O/C (**Figure 5a**) shows that the evap samples are characterized by high ratios, because of polystyrene screening by a thick residue of evaporation. Exceptions are related to the variability explained above. More interesting, it appears that the same relationship is followed by all samples (UFch, native, and UCch; evap, ads, and rins), indicating that the analyzed organic compounds all have the same N/O ratio equal to about 0.17.

In order to gain deeper insight into the chemical nature of these compounds, the C_{1s} peak was decomposed into 4 components following the procedure used before for materials of biological origin (food products (*14*), biochemical model compounds (*18*), and microorganisms (*32*, *33*)): no constraint on position, except for the C-(C, H) component set at 284.8 eV; full width at half-maximum (fwhm) imposed to be the same for all 4 components. Note that the spectral window shown in **Figure 4** includes the

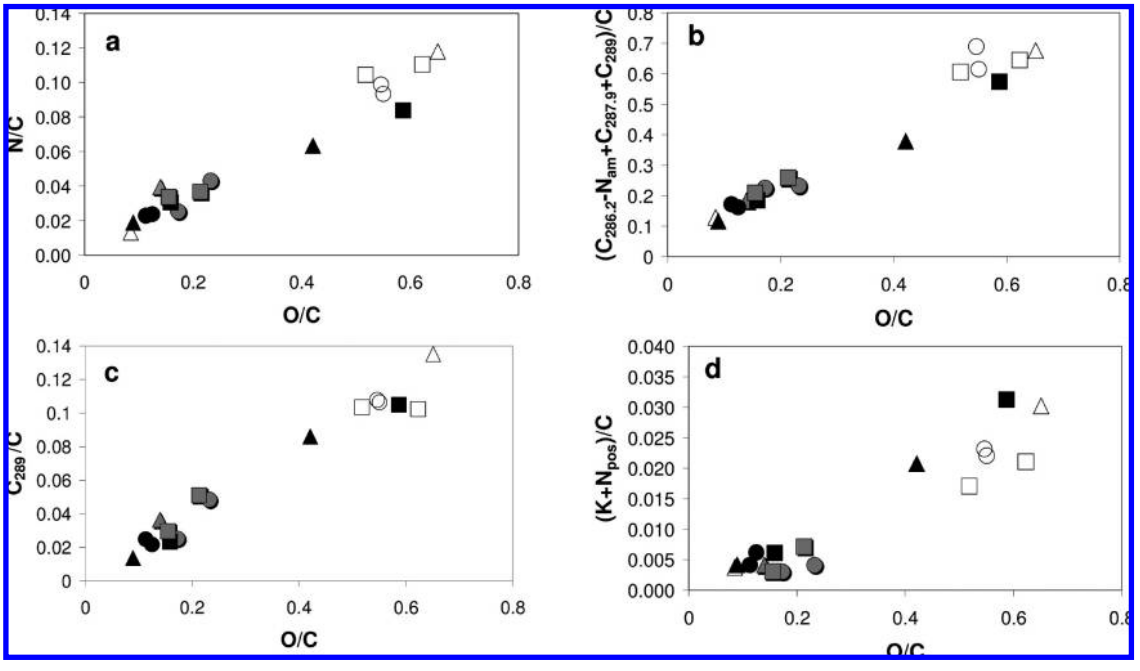

Figure 5. Plot of molar concentrations, ratioed to total carbon, versus the oxygen to carbon molar ratio: (**a**) total nitrogen, (**b**) carbon bound to a heteroatom minus nitrogen of amine or amide type, (**c**) carbon responsible for the C_{1s} component at 289 eV, and (**d**) potassium plus positively charged nitrogen. Polystyrene conditioned with UFch (triangles), native (circles), and UCch (squares) champagne following procedures evap (open symbols), ads (black symbols), and rins (gray symbols).

K_{2p} doublet and a weak C_{1s} satellite (shake up) due to polystyrene, depending on the sample. The N_{1s} peak was decomposed into 2 components, the fwhm of which was imposed to be same. **Figure 4** illustrates these decompositions. The O_{1s} peak was not decomposed because of a lack of detailed features and of visible variations. The list of the components of the C_{1s} and N_{1s} peaks with their approximate position and their assignment is given in **Table 2**. The binding energy expected for oxygen in different chemical functions is also given. The molar concentrations of the elements responsible for the different components, ratioed to the total carbon concentration, are given in **Table 1**.

According to the assignment of the C_{1s} peak components, the oxygen concentration is expected to be equal to the balance of the concentrations $[C_{286.2} - N_{am} + C_{287.9} + C_{289}]$. **Figure 5b** shows that a relationship close to 1:1 is indeed observed. The deviation is not significant, taking account of the experimental variability and of the uncertainty affecting the O_{1s} sensitivity factor (*13*, *34*). For the same reason, it is not justified to attempt refining the balance to account more specifically for the presence of acetal (3 carbon atoms bound to 2 oxygen atoms) and of carboxylate or carboxyl (2 oxygen bound to 1 carbon). In order to ensure that there was no important bias due to the C_{1s} peak decomposition procedure, another procedure has also been used: no constraint on the fwhm of the 284.8 eV component, fwhm of the 3 other components imposed to be the same, and position of these 3 components imposed to be close to mean value found for evap samples, i.e., 286.2, 287.9, and 289.0 eV. This alternative decomposition procedure gave a lower fwhm and a lower intensity for the C-(C,H) component, and a higher intensity for the C-(O,N) component. The plot (not shown) analogous to **Figure 5b** is simply shifted by about 0.07 units to higher ordinate values. **Figure 5c** demonstrates that the C_{289}/C ratio is proportional to the O/C ratio with a C_{289}/O ratio equal to about 0.19. **Figure 5d** shows that the $(K + N_{pos})/C$ ratio is also linearly related with the O/C ratio. The slope provides a $(K + N_{pos})/O$ ratio equal to about 0.05 in which positively charged nitrogen is dominating with respect to potassium.

The XPS data were also examined regarding the chemical functions containing nitrogen. If neutral nitrogen is due to amide, then its concentration is expected to be equal to the concentration of carbon responsible for the C_{1s} component at 287.9 eV, from which the contribution of acetal is subtracted. The latter can be evaluated by the following relationship (*14*):

$$C_{ac}/C = 0.2[C_{286.2} - N]/C \quad (4)$$

based on the assumption that the $C_{286.2}$ component is due to either C-O or C-N and that the concentration of C-O due to compounds other than carbohydrates is negligible, and considering one acetal or hemiacetal per hexose unit in carbohydrates. The plot of $(C_{287.9} - C_{ac})/C$ versus N_{am}/C is shown in **Figure 6**. A clear correlation is obtained, and the slope given by most of the results is close to unity. An analogous plot (not shown) performed with data obtained using the alternative decomposition procedure of the C_{1s} peak described above gives the same slope but is shifted by 0.015 to lower ordinate values. This is the consequence of an overestimation of the $C_{286.2}$ component by this alternative procedure. **Figure 6** thus supports the attribution of the main N_{1s} component near 400.0 eV to amide functions, presumably the peptidic link. Accordingly, it may be taken as a marker either of amide derivatives of polysaccharides or of polypeptides.

DISCUSSION

The results of this work are relevant to the nature of the champagne adlayer regarding its general organization, its

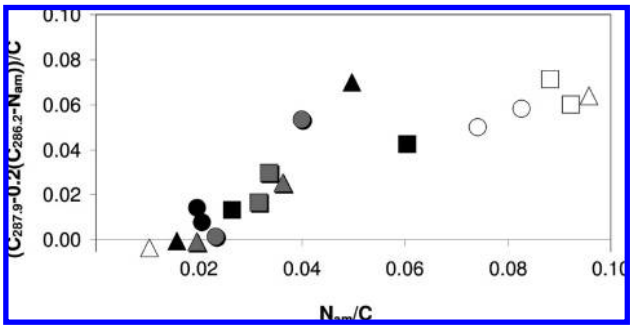

Figure 6. Plot of the molar concentrations ratioed to total carbon: carbon making two single bonds or a double bond with oxygen minus carbon of acetal or hemiacetal vs nitrogen of amide or amine. Polystyrene conditioned with UFch (triangles), native (circles), and UCch (squares) champagne following procedures evap (open symbols), ads (black symbols), and rins (gray symbols).

macromolecular composition, and the occurrence of certain chemical functions.

The geometry of the adlayer is typically that of a domain structured layer. The layer adsorbed or deposited on polystyrene is heterogeneous. This is shown by the fluctuating signal evolutions measured by ellipsometry (**Figure 1**) and by the domain structure observed by Brewster angle microscopy (**Figure 3**) (*9*, *31*). The size of these domains may be larger than the area (480 × 640 μm) analyzed by optical microscopy (*35*, *36*). This was revealed by some black holes in BAM images (**Figure 3**), which may be related to lower molar concentration ratios (particularly with Ufch samples) and a high variability in the XPS data (**Table 2**). Nevertheless, **Figure 5** shows that the organic constituents of champagne analyzed on polystyrene are similar regarding the concentration of total nitrogen, total oxygen, oxygen-bearing functions (C−O, C═O, and O═C−O), and cations, without any significant influence either of ultrafiltration or of the procedure of deposition on polystyrene (evaporation, adsorption, and adsorption + rinsing) (**Figure 5**). It further shows that rinsing does not drastically decrease the surface concentration of these compounds, which indicates that they are strongly adsorbed on polystyrene. Some experimental data show even a higher concentration as a result of rinsing. This is hardly significant in view of the low values and their limited precision; however, it might be related to the fact that adsorption and drying (ads) leaves an adsorbed layer with a domain structure (**Figure 3**), while rinsing may allow the adlayer to spread out and more homogeneously cover the polystyrene surface.

The macromolecular composition of the adlayer may be evaluated by comparing its elemental composition with that of model compounds. The model compounds to be considered are proteins or polysaccharides, according to the chemical composition of wines. The analysis of the polypeptides in champagne is under way (*37*), but an important grape protein found in wine is invertase (*11*), the amino acid composition of which is known (**Table 3**). Proteins have often been suspected to play an important role in the foam behavior of champagne (*38*, *39*). In contrast, the adsorption of polysaccharides in champagne has been less studied (*40*). Some polysaccharides were characterized recently for white wines produced from Loureiro grapes (*41*) or for the Portuguese Bairrada appellation (*42*). The polysaccharides originate both from grape and microorganisms. Pectic polysaccharides (rhamnogalacturonan II, molar mass ~10 kDa; galacturonans) and proteoglycans (arabinogalactan proteins, molar mass ~150 kDa) arise from grape berry after degradation by pectinases during the maturation of grape and during the

Table 3. Concentration of Macromolecular Compounds in Champagne, Chemical Composition of Model Compounds (Molar Ratio of Elements and Carbon Concentration), and Relative Concentration of Model Compounds in the Champagne Constituents Present on Polystyrene (C_i/C and Weight %)

		composition of i				conc. of i in the adlayer	
model constituent, i	conc. of i in champagne (mg L^{-1})[c]	O/C	N/C	O/N	carbon conc. (mmol/g)	C_i/C	wt %
protein[a]	5−10	0.303	0.240	1.259	45	0.41	35
polysaccharides[b]	200−500	0.833	0		37	0.63	65

[a] From the amino acid sequence of the grape invertase (accession number Q9S943), which represents 9 to 14% of the total protein content of a Chardonnay wine. Element formula $C_{4.16}H_{7.47}O_{1.26}N_1S_{0.02}$ is expressed with respect to one nitrogen atom. [b] Polysaccharide, $(C_6H_{10}O_5)_n$. [c] Data are from ref 7.

first steps of wine making (*42*). Mannans and mannoproteins, with molar masses between 53 and 560 kDa, arise from yeast during and after fermentation (*41*). The fractionation of these polysaccharides shows that they usually contain less than 10% (w/w) protein (*43*).

As pointed out in the Results section, the XPS signal may originate partly from the polystyrene substrate. This affects the reproducibility and accuracy of individual results but does not prevent the extraction of information from the correlations shown in **Figures 5** and **6**. **Figure 5a** shows that the N/O molar ratio is 0.174 (s.d. 0.005), which indicates that the samples only differ significantly by the importance of the polystyrene contribution. The highest N/C and O/C ratios, 0.12 and 0.65, respectively, correspond to a situation where the champagne constituents are practically completely screening the polystyrene signal. In the surface composition, N_{am} represents about 82% of total nitrogen (**Table 1**). Let us assume that N_{am} is due to proteins characterized by a N/C ratio of 0.240, calculated from amino acid composition of a major champagne protein (**Table 3**). Thus,

$$N_{am}/C = 0.12 \times 0.82 = 0.240(C_{Pr}/C) \quad (5)$$

where C_{Pr}/C is the proportion of carbon in the form of protein in the adlayer.

Accordingly C_{Pr}/C = 0.41, which means that proteins account for 41% of the total carbon of the adlayer. Moving now to the oxygen peak, let us assume that it comes from proteins or from sugars of glycoproteins or other macromolecules. In proteins and in polysaccharides, the O/C ratios are 0.303 and 0.833, respectively (**Table 3**). Thus,

$$O/C = 0.65 = 0.303(C_{Pr}/C) + 0.833(C_{PS}/C) \quad (6)$$

where C_{PS}/C is the proportion of carbon in the form of polysaccharide in the adlayer. Using the calculated C_{Pr}/C value, we can determine that C_{PS}/C = 0.63. Dividing C_{Pr}/C and C_{PS}/C by the carbon concentration in the relevant compound (**Table 3**), we can provide the ratio of the weight of the constituents, protein and polysaccharide, over the total concentration of carbon (*14*). Dividing each ratio by the sum of the ratios, we can finally give the weight fraction of protein and polysaccharide in the volume probed by XPS. At this stage of the analysis, it appears that the adlayer comprises approximately 35% protein and 65% polysaccharide (w/w).

For grape invertase, taken as the model protein, the proportion of carbon only bound to carbon and hydrogen is expected to be equal to 1 − O/C − N/C − S/C = 0.46 (**Table 3**). Accordingly, the proportion of carbon only bound to carbon and hydrogen in the adlayer proteins is expected to be 0.41 × 0.46 = 0.19. **Table 1** shows that the overall proportion is in the range 0.22 to 0.31 when the champagne constituents are practically completely screening the signal of polystyrene (samples of the upper right corner in **Figure 5a**). This indicates that the proportion of carbon in the form of hydrocarbon does not exceed about 0.1 and that lipids are not present in appreciable concentration. The XPS analysis of food products and complex mixtures of biochemical compounds has revealed the tendency of lipids to migrate to the surface, with respect to proteins and polysaccharides (*14*−*17*), the driving force being the decrease of surface energy. While the occurrence of minor components may not be ruled out, it may thus be concluded that the surface active compounds of champagne are mostly constituted of proteins and polysaccharides in a ratio of the order of 35:65 and do not contain an appreciable proportion of lipids, or more generally of hydrocarbon chains.

It is striking that **Figures 5** and **6**, concerning the polystyrene/liquid interface, do not show any significant differences between samples originating from ultrafiltrate, native, and ultraconcentrate base wines, in contrast with data concerning the air/liquid interface (**Figures 1** and **2**). This may be due to the limited reproducibility of XPS results. Moreover, the heterogeneous character of the adlayer on polystyrene (**Figure 3**) decreases the sensitivity of XPS to the adlayer average thickness. However, the nature of the surface active compounds leads us to raise the hypothesis that the adlayer may be formed not only by adsorption of macromolecules (molar mass > 10 000), sensu stricto, but also by association of smaller molecules of proteic and polysaccharidic nature, especially in the case of ultrafiltrated champagne.

For samples covered by a thick adlayer (**Figure 5c**, upper symbols), the XPS signals also give information on particular chemical functions occurring in the adlayer. The carboxyl groups or esters, responsible for the C_{1s} component at 289.0 eV, represent about 11% of total carbon, i.e., about 18% of carbon due to nonpolypeptidic compounds. The carboxyl groups or esters can be linked to the presence of uronic acids (such as D-galacturonic and D-glucuronic acids) in pectic polysaccharides originated from grapes (*44*), from combinations of polyphenols with tartaric acid such as hydroxycinnamic tartaric esters (*45*), or from complexes of fatty-acids with glucides (*46*). According to the above data, pectic polysaccharides are the most probable. Finally, the plot of the $(K + N_{pos})/C$ versus O/C (**Figure 5**) shows that the concentration of the cations, N_{pos} and K^+, is not markedly influenced by the sample preparation procedure when a thick adlayer is present. This strongly supports the idea that these cations are associated with the macromolecules. N_{pos} may be due to basic amino acids, to amino sugars, or to ammonium acting as a counterion of carboxylate. The latter attribution is also valid for the traces of potassium.

To conclude, the XPS analysis of both adsorbed layers and deposits of champagne shows that the nonvolatile organic compounds are mainly made of proteins and polysaccharides. A tentative explanation is that these compounds tend to self-assemble in the liquid phase, forming larger size moieties, and/or at interfaces either with air or with polystyrene. This interpretation is in agreement with previous studies which have demonstrated that the macromolecular fraction isolated by ultrafiltration (with a nominal molar mass molar cutoff of 10^4) is of polysaccharidic nature with a less abundant protein fraction (31% w/w), as evaluated by NMR and chemical analysis (*40*). Nevertheless, the respective roles of these compounds still need to be understood.

ACKNOWLEDGMENT

We thank C. Bliard and M. Genet for fruitful discussions.

LITERATURE CITED

(1) Liger-Belair, G.; Voisin, C.; Jeandet, P. Modeling Nonclassical heterogeneous bubble nucleation from cellulose fibers: Application to bubbling in carbonated beverages. *J. Phys. Chem. B* **2005**, *109* (30), 14573–14580.

(2) Douillard, R.; Liger-Belair, G.; Puff, N.; Aguié-Béghin, V. Les bulles et la Mousse du Champagne. Un peu de Physique. *Le Vigneron Champenois* **2000**, *6*, 50–65.

(3) Machet, F.; Robillard, B.; Duteurtre, B. Application of image analysis to foam stability of sparkling wines. *Sci. Aliments* **1993**, *13*, 73–87.

(4) Liger-Belair, G. The Physics and chemistry behind the bubbling properties of champagne and sparkling wines: A state-of-the-art review. *J. Agric. Food Chem.* **2005**, *53* (8), 2788–2802.

(5) Péron, N.; Cagna, A.; Valade, M.; Bliard, C.; Aguié-Béghin, V.; Douillard, R. Layers of macromolecules at the champagne/air interface and the stability of champagne bubbles. *Langmuir* **2001**, *17*, 791–797.

(6) Lucassen, J. Dynamic Properties of Free Liquid Films and Foams. Anionic Surfactants: Physical Chemistry of Surfactant Action. In *Surfactant Science Series*; Schick, M. J., Fowkes, F. M., Ed.; Marcel Dekker: New York, 1981; Vol. *11*, pp 217−265.

(7) Tusseau, D.; van Laer, S. Etude des macromolécules des vins de champagne. *Sci. Aliments* **1993**, *13*, 463–482.

(8) Brissonnet, F.; Maujean, A. Characterization of foaming proteins in a champagne base wine. *Am. J. Enol. Vitic.* **1993**, *44* (3), 297–301.

(9) Péron, N.; Meunier, J.; Cagna, A.; Valade, M.; Douillard, R. Phase separation in molecular layers of macromolecules at the champagne-air interface. *J. Microsc.* (*Oxfod, U.K.*) **2004**, *214*, 89–98.

(10) Brissonnet, F.; Maujean, A. Identification of some foam-active compounds in champagne base wines. *Am. J. Enol. Vitic.* **1991**, *42* (2), 97–102.

(11) Marchal, R.; Bouquelet, S.; Maujean, A. Purification and partial biochemical characterization of glycoproteins in a Champenois Chardonnay wine. *J. Agric. Food Chem.* **1996**, *44* (7), 1716–1722.

(12) Puff, N.; Marchal, R.; Aguié-Béghin, V.; Douillard, R. Is grape invertase a major component of the adsorption layer formed at the air/champagne wine interface. *Langmuir* **2001**, *17*, 2206–2212.

(13) Genet, M. J.; Dupont-Gillain, C. C.; Rouxhet, P. G. XPS Analysis of Biosystems and Biomaterials. In *Medical Applications of Colloids*; Matijevic, E., Ed.; Springer: New York, 2008; pp 177−307.

(14) Rouxhet, P. G.; Misselyn-Bauduin, A. M.; Ahimou, F.; Genet, M. J.; Adriaensen, Y.; Desille, T.; Bodson, P.; Deroanne, C. XPS analysis of food products: toward chemical functions and molecular compounds. *Surf. Interface Anal.* **2008**, *40* (3−4), 718–724.

(15) Bosquillon, C.; Rouxhet, P.; Ahimou, F.; Simon, D.; Culot, C.; Préat, V.; Vanbever, R. Aerosolization properties, surface composition and physical state of spray-dried protein powders. *J. Controlled Release* **2004**, *99*, 357–367.

(16) Gaiani, C.; Ehrhardt, J. J.; Scher, J.; Hardy, J.; Desobry, S.; Banon, S. Surface composition of dairy powders observed by X-ray photoelectron spectroscopy and effects on their rehydration properties. *Colloids Surf., B* **2006**, *49*, 71–78.

(17) Gaiani, C.; Scher, J.; Ehrhardt, J. J.; Linder, M.; Schuck, P.; Desobry, S.; Banon, S. Relationships between dairy powder surface composition and wetting properties during storage: importance of residual lipids. *J. Agric. Food Chem.* **2007**, *55*, 6561–6567.

(18) Gerin, P. A.; Dengis, P. B.; Rouxhet, P. G. Performance of XPS analysis of model biochemical compounds. *J. Chim. Phys.* **1995**, *92* (5), 1043–1065.

(19) Drude, P. Reflexion und brechung bei oberflâchenschichten. *Ann. Phys. Chem.* (*Leipzig*) **1891**, *43*, 126–157.

(20) Meunier, J. Liquid interfaces: role of the fluctuations and analysis of ellipsometry and reflectivity measurements. *J. Phys.* (*Paris*) **1987**, *48*, 1819–1831.

(21) Azzam, R. M. A.; Bashara, N. M. *Ellipsometry and Polarized Light*; North Holland: Amsterdam, 1987.

(22) Abdallah, Z.; Aguié-Béghin, V.; Abou Saleh, K.; Douillard, R.; Bliard, C. Isolation, purification and analysis of the macromolecular fractions responsible for the surface properties in native Champagne wines, submitted for publication.

(23) Liger-Belair, G.; Religieux, J. B.; Fohanno, S.; Vialatte, M. A.; Jeandet, P.; Polidori, G. Visualization of mixing flow phenomena in Champagne glasses under variuos glass-shape and engravement conditions. *J. Agric. Food Chem.* **2007**, *55*, 882–888.

(24) Labourdenne, S.; Gaudry-Rolland, N.; Letellier, S.; Lin, M.; Cagna, A.; Esposito, G.; Verger, R.; Rivière, C. The oil-drop tensiometer: potential applications for studying the kinetics of (phospho)lipase action. *Chem. Phys. Lipids* **1994**, *71*, 163–173.

(25) Benjamins, J.; Cagna, A.; Lucassen-Reynders, E. H. Viscoelastic properties of triacylglycerol-water interfaces covered by proteins. *Colloids Surf.* **1996**, *114*, 245–254.

(26) Péron, N.; Cagna, A.; Valade, M.; Marchal, R.; Maujean, A.; Robillard, B.; Aguié-Béghin, V.; Douillard, R. Characterization by drop tensiometry and by ellipsometry of the adsorption layer formed at the air/champagne wine interface. *Adv. Colloid Interface Sci.* **2000**, *88*, 19–36.

(27) Sausse, P.; Aguié-Béghin, V.; Douillard, R. Effects of epigallocatechin gallate on beta-casein adsorption at the air/water interface. *Langmuir* **2003**, *19*, 737–743.

(28) Hambardzumyan, A.; Aguié-Béghin, V.; Douillard, R. β-Casein and symmetrical triblock copolymer (PEO-PPO-PEO and PPO-PEO-PPO) surface properties at the air-water interface. *Langmuir* **2004**, *20*, 756–763.

(29) Harke, M.; Stelzle, M.; Motschmann, H. R. Microscopic ellipsometry: imaging monolayer on arbitrary reflecting supports. *Thin Solid Films* **1996**, *284−285*, 412–416.

(30) Harke, M.; Teppner, R.; Schulz, O.; Motschmann, H.; Orendi, H. Description of a single modular optical setup for ellipsometry, surface plasmons, waveguide modes, and their corresponding imaging techniques including Brewster angle microscopy. *Rev. Sci. Instrum.* **1997**, *68* (8), 3130–3134.

(31) Abou Saleh, K.; Aguié-Béghin, V.; Foulon, L.; Valade, M.; Douillard, R. Characterization by optical measurements of the effects of some stages of champagne technology on the adsorption layer formed at the gas/wine interface. *Langmuir* **2007**, *23* (13), 7200–7208.

(32) Boonaert, C. J. P.; Rouxhet, P. G. Surface of lactic acid bacteria: relationships between chemical composition and physicochemical properties. *Appl. Environ. Microbiol.* **2000**, *66* (6), 2548–2554.

(33) Ahimou, F.; Boonaert, C. J. P.; Adriaensen, Y.; Jacques, P.; Thonart, P.; Paquot, M.; Rouxhet, P. G. XPS analysis of chemical functions at the surface of *Bacillus subtilis*. *J. Colloid Interface Sci.* **2007**, *309* (1), 49–55.

(34) Briggs, D.; Fairley, N. XPS of chemically modified low intensity polyethylene surfaces: observations on curve fitting the C 1s spectrum. *Surf. Interface Anal.* **2002**, *33*, 283–290.

(35) Mann, E. K.; Lee, L. T.; Hénon, S.; Langevin, D.; Meunier, J. Polymer-surfactant films at the air-water interface. 1. Surface pressure; ellipsometry, and microscopic studies. *Macromolecules* **1993**, *26*, 7037–7045.

(36) Abou Saleh, K.; Aguié-Béghin, V.; Foulon, L.; Valade, M.; Douillard, R. Relations between the air/wine adsorption layer and the bubble collar stability in experimental and commercial champagnes. *Colloids Surf., A* **2009**, *334*, 86–96.

(37) Cilindre, C.; Jégou, S.; Hovasse, A.; Schaeffer, C.; Castro, A. J.; Clément, C.; Van Dorsselaer, A.; Jeandet, P.; Marchal, R. Proteomic approach to identify champagne wine proteins as modified by botrytis cinerea infection. *J. Proteome Res.* **2008**, *7*, 1199–1208.

(38) Malvy, J.; Robillard, B.; Duteurtre, B. Influence of proteins on the foam behavior of champagne wines. *Sci. Aliments* **1993**, *14*, 87–98.

(39) Dambrouck, T.; Marchal, R.; Cilindre, C.; Parmentier, M.; Jeandet, P. Determination of the grape invertase content (using Pta-Elisa) following various fining treatments versus changes in the total protein content of wine. Relationships with wine foamability. *J. Agric. Food Chem.* **2005**, *53*, 8782–8789.

(40) Abdallah, Z.; Aguié, V.; Douillard, R.; Bliard, C. Champagne Bubbles: Isolation and Characterization of Amphiphilic Macromolecules Responsible for the Stability of the Collar at the

Champagne /Air Interface. In *Macromolecules and Secondary Metabolites of Grapewine and Wines*; Clement C., Jeandet P., Eds.; Lavoisier: Paris, France, 2006.

(41) Gonçalves, F.; Heyraud, A.; Norberta de Pinho, M.; Rinaudo, M. Characterization of white wine mannoproteins. *J. Agric. Food Chem.* **2002**, *50* (21), 6097–6101.

(42) Coimbra, M. A.; Goncalves, F.; Barros, A. S.; Delgadillo, I. Fourier transform infrared spectroscopy and chemometric analysis of white wine polysaccharide extracts. *J. Agric. Food Chem.* **2002**, *50* (12), 3405–3411.

(43) Pellerin, P.; Vidal, S.; Williams, P.; Brillouet, J. M. Characterization of five type II arabinogalactan-protein fractions from red wine of increasing uronic acid content. *Carbohydr. Res.* **1995**, *277*, 135–143.

(44) Doco, T.; Brillouet, J. M. Isolation and characterization of a rhamnogalacturonan II from red wine. *Carbohydr. Res.* **1993**, *243* (2), 333–343.

(45) Chamkha, M.; Cathala, B.; Cheynier, V.; Douillard, R. Phenolic Composition of champagnes from Chardonnay and Pinot Noir vintages. *J. Agric. Food Chem.* **2003**, *51* (10), 3179–3184.

(46) Flanzy, C. *Oenologie: Fondements Scientifiques et Technologiques*; Lavoisier: Paris, France, 1998; p 1311.

Received May 25, 2009. Revised manuscript received September 2, 2009. Accepted September 2, 2009. The support of National Foundation for Scientific Research (F.N.R.S., Belgium) is gratefully acknowledged.